

AKARI slit-less spectroscopy and broadband infrared photometry observations of Hickson Compact Groups 56 and 92

AYATO IKEUCHI,¹ ITSUKI SAKON,¹ TAKASHI ONAKA,¹ FRÉDÉRIC GALLIANO,^{2,3} AND RONIN WU⁴

¹*Department of Astronomy, Graduate School of Science, The University of Tokyo, 7-3-1 Hongo, Bunkyo-ku, Tokyo 113-0033, Japan*

²*IRFU, CEA, Université Paris-Saclay, F-91191 Gif-sur-Yvette, France*

³*Université Paris-Diderot, AIM, Sorbonne Paris Cité, CEA, CNRS, F-91191 Gif-sur-Yvette, France*

⁴*LERMA, Observatoire de Paris, PSL Research University, CNRS, Sorbonne Univrsite, UPMC Paris 06, 92190, Meudon, France*

ABSTRACT

Based on near- to far-infrared spectral energy distribution (SED) analyses, we have investigated star-formation activities of galaxies in Hickson Compact Groups (HCGs) that indicate clear signs of interactions. The study provides us information on the effects of interactions on the galactic environments of member galaxies and their evolution. We combined *AKARI* slit-less 2–14 μm spectra and 3–24 μm medium-band image datasets of HCG 56 and 92, both of which show ongoing interactions, and made a comparison of the observed near- to far-infrared SEDs with the latest SED models of star-forming galaxies and AGNs. We estimated the star-formation rates (SFRs) of the member galaxies via two different methods; i) using the mid-infrared UIR band strength and ii) using the far-infrared luminosity originating from star-formation estimated from the SED model. We found a discrepancy between the SFRs derived from the two methods, in particular for the galaxies that harbor AGNs. We interpreted that this discrepancy could be due to the possible destruction of the carriers of the Unidentified InfraRed (UIR) bands in galaxies with AGNs. In the star formation rate versus stellar mass diagram, all galaxies in HCG 56 and 92 galaxies are distributed below the main sequence of the star-forming SDSS field galaxies. We conclude that the enhanced star-formation due to galaxy interactions is not seen in HCG 56 and 92, or that the star-formation seems to be rather suppressed in these groups.

Keywords: Interacting galaxies, Local Universe, Galaxy evolution, ISM

1. INTRODUCTION

Compact groups are suitable targets to investigate the effects of interactions on the galactic environments of member galaxies and their evolution because they relatively have low velocity dispersions unlike galaxy clusters, which indicates the gravitational interactions among the member galaxies. [Hickson \(1982\)](#) made a catalog of compact groups with Palomar Observatory Sky Survey. He identified 100 groups based on galaxy population (N ; the number of galaxies in a group ≥ 4), isolation ($\theta_N \geq 3\theta_G$) and compactness ($\mu_G \leq 26.0$). A large fraction of his catalog is still thought to be real groups. We investigated two groups of Hickson Compact Groups (Hereafter HCGs), HCG 56 and 92 based on near- to mid-infrared imaging and spectroscopic observations. Both groups have an active galaxy ([Véron-Cetty & Véron 2006](#)), galaxies that have disturbed morphology and a bridge structure. Thus, these groups exhibit the signs of strong interaction in spite of their short dynamical lifetime ($\sim 10^9$ yr, [Rubin et al. 1990](#)), and provide us opportunities to investigate the effects of close interactions among the galaxies on the galactic environments. Interstellar dust plays a key role to perceive the galactic environments since it determines the spectrum of galaxies by absorbing ultraviolet to optical photons from the heating sources and by re-radiating in the infrared wavelengths. We collected *AKARI*, *Spitzer*, and *Herschel* datasets to reproduce the whole infrared shape of SED both for HCG 56 and 92.

2. TARGETS AND DATASETS

Near- and mid-infrared slit-less spectroscopic observations of HCGs have been carried out in the *AKARI* open time program SHARP (PI: Itsuki Sakon). In addition, near-, mid- and far-infrared imaging observations of HCGs have been carried out with *AKARI*/IRC ([Onaka et al. 2007](#)) and *AKARI*/FIS ([Kawada et al. 2007](#)) in the Mission Program ISMGN (PI: Hidehiro Kaneda). For image datasets, we analyzed on the IRC datasets calibrated by [Egusa et al. \(2016\)](#). We

performed reduction on the raw spectroscopic datasets of *AKARI*/IRC with our own reduction tool to gain individual spectra of galaxies. We carefully extracted the spectra in the same aperture as photometry and deconvolved the spectral-overlapping with other member galaxies. In the far infrared wavelengths, the spatial resolution achieved by the *AKARI*/FIS was insufficient to resolve the member galaxies and, therefore, the *AKARI*/FIS datasets were not used in the following discussion. In addition to *AKARI* datasets, we retrieved archival image datasets of *Spitzer* and *Herschel* telescope. We used IRAC (Fazio et al. 2004) and MIPS (Rieke et al. 2004) datasets of *Spitzer*, and used PACS (Poglitsch et al. 2010) and SPIRE (Griffin et al. 2010) datasets of *Herschel*. Because of the spatial resolution, we used PACS and SPIRE data for the far-infrared instead of the FIS data. These datasets were already calibrated by each telescope’s pipeline.

2.1. HCG 56

HCG 56 has five member galaxies (HCG 56a-e; see Figure 1). The typical redshift of HCG 56 is 0.0270 (~120 Mpc). HCG 56b is categorized into Seyfert 1 (Véron-Cetty & Véron 2006). We have extracted near- to mid-infrared spectra and constructed infrared photometric SEDs of HCG 56a, b, d and e using *AKARI* datasets (pointing ID: 1402230.1, 1402231.1 and 3220004.1), *Spitzer* datasets (AORKEY: 23026944 and 23031296) and *Herschel* datasets (observation ID: 134255878). HCG56c is very faint in the mid- to far-infrared and is located very close to HCG56d. The possible cause of faintness in mid- to far-infrared wavelengths in HCG 56c is the sputtering of the dust due to the strong interaction with HCG 56b. Therefore, HCG 56c is not included in the following discussion. Figure 2 is an example of photometric and spectroscopic SED with our datasets. This galaxy is HCG 56a.

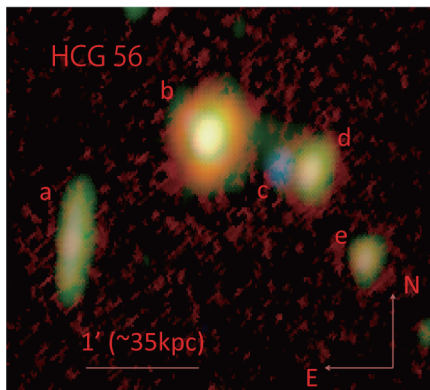


Figure 1. An *AKARI*/IRC composite image of HCG 56 with our dataset. (blue; N3(3.2 μm) green; S11(11 μm) red; L24(24 μm)

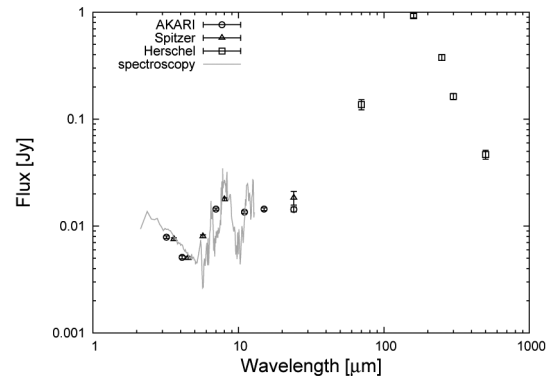


Figure 2. The photometric and spectroscopic SED of HCG 56a in observed frame. The open circles, triangles and squares represent the photometric values of *AKARI*, *Spitzer* and *Herschel* bands, respectively. The spectrum extracted from the *AKARI* slit-less observation is also shown with the grey line.

2.2. HCG 92

HCG 92 is known as Stephan’s Quintet. HCG 92 has five member galaxies (HCG 92a-e), and HCG 92a is thought to be a foreground galaxy and the distance is estimated as ~14 Mpc. The typical redshift of HCG 56 is 0.0225 (~70 Mpc). HCG 92c is categorized into Seyfert 2 (Véron-Cetty & Véron 2006). We also analyzed two starbursts which had been identified by ISO/ISOCAM in the HCG 92 system, SQ-A and SQ-B. Finally, we successfully extracted spectra of HCG 92a, c and SQ-B. We could not extract 92b and d spectra because these galaxies have close spatial location and complicated morphology originating from the interaction. We also constructed photometric SEDs for HCG 92a, b+d, c, e, SQ-A and SQ-B using the *AKARI* datasets (pointing ID: 1402236.1, 3220003.1, and 3221001.1), the *Spitzer* datasets (AORKEY: 6011392 and 22393616) and the *Herschel* datasets (observation ID: 1342245660 and 1342220635).

3. STAR-FORMATION RATES

We compared SFR derived from i) Unidentified InfraRed (UIR) band strengths and ii) FIR luminosity (8–1000 μm) based on the latest infrared dust models of each galaxies. We used equations referred to Shipley et al. (2016) for comparison of two methods. This provided us to use the same initial mass function (Kroupa IMF) and direct comparison.

3.1. SFR derived from UIR band strengths

We measured the strength of UIR 6.2 μm ($L_{\text{UIR}6.2\mu\text{m}}$) feature by integrating the flux over the polynomial continuum through continuum points at 5.9 μm and 6.6 μm of the obtained spectra. After integration, we estimated SFRs by using follow equation (Shipley et al. 2016, eq. (11))

$$\text{SFR}_{6.2\mu\text{m}} [M_{\odot}/\text{yr}] = 10^{-40.06+0.96 \log_{10}(L_{\text{UIR}6.2\mu\text{m}} [\text{erg/s}])}$$

3.2. SFR derived from the FIR luminosity

We constructed SED models for all galaxies that have photometric data. We fitted two different starburst dust models (AC model (Galliano et al. 2011) and THEMIS model (Jones et al. 2013) to investigate the dependence on the dust properties. For AGN harbors (HCG 56b and 92c), we added an AGN template of Siebenmorgen et al. (2015) in linear combination to the dust model. Then, we integrated 8–1000 μm luminosity ($L_{8-1000\mu\text{m}}$) of each SED model and converted it into SFRs via the following equation (Shipley et al. 2016, eq. (20)). Excluding the AGN component, only dust component was used to calculate the SFRs for the AGN hosts,

$$\text{SFR}_{\text{FIR}} [M_{\odot}/\text{yr}] = 2.54 \times 10^{-44} L_{8-1000\mu\text{m}} [\text{erg/s}].$$

4. RESULTS AND DISCUSSION

The calculated SFR is summarized in Table 1. For convenience, we included the results of Bitsakis et al. (2011) obtained from the MAGPHYS (da Cunha et al. 2008, Chabrier IMF) in the table. We can recognize clearly that $\text{SFR}_{6.2\mu\text{m}}$, SFR_{FIR} and $\text{SFR}_{\text{MAGPHYS}}$ are roughly consistent with each other in the normal star-forming galaxies. A similar trend is also found in $\text{SFR}_{6.2\mu\text{m}}$ and $\text{SFR}_{\text{MAGPHYS}}$ of the AGN host galaxies (HCG 56b and 92c; see Table 1). On the other hand, discrepancy of an order magnitude is found between $\text{SFR}_{6.2\mu\text{m}}$ and SFR_{FIR} . This implies that the dust composition and/or the dust size distribution might be changed in AGN host galaxies. We also compared our results with the Galactic SFR (Robitaille & Whitney 2010) and the star-formation main sequence of nearby galaxies ($z \sim 0.1$, Brinchmann et al. 2004). We found that our samples are always distributed below the SFR vs. M_{\star} relation (Figure 3) obtained by Brinchmann et al. (2004) and not significantly higher than the Galactic SFR (0.68–1.45 M_{\odot}/yr , Robitaille & Whitney 2010). Hence, we concluded that the enhanced star-formation due to galaxy interactions is not seen in HCG 56 and 92, or that the star-formation seems to be even suppressed in these groups on the contrary.

Table 1. Star-formation rates derived from different methods.

	$\text{SFR}_{6.2\mu\text{m}} [M_{\odot}/\text{yr}]$	$\text{SFR}_{\text{FIR}}^{\text{AC}} [M_{\odot}/\text{yr}]$	$\text{SFR}_{\text{FIR}}^{\text{THEMIS}} [M_{\odot}/\text{yr}]$	$\text{SFR}_{\text{MAGPHYS}} [M_{\odot}/\text{yr}]$	$M_{\star} [\times 10^9 M_{\odot}]$	starburst component [%]
	(1)	(2)	(3)	(4)	(5)	(6)
HCG 56a	0.64±0.07	1.17±0.06	1.26±0.06	0.57±0.23	17.78	100
HCG 56b	0.03±0.02	0.32±0.02	0.26±0.01	0.13±0.05	34.67	13.1 (AC) & 10.5 (THEMIS)
HCG 56d	0.90±0.04	0.98±0.05	0.99±0.05	0.40±0.16	10.23	100
HCG 56e	0.17±0.08	0.34±0.02	0.34±0.02	0.24±0.10	4.29	100
HCG 92a	0.03±0.01	0.06±0.01	0.06±0.01	-	11.75	100
HCG 92b+d	-	0.59±0.03	0.59±0.03	0.57±0.23	72.69	100
HCG 92c	0.04±0.01	0.78±0.04	0.76±0.04	0.08±0.03	39.81	42.3 (AC) & 39.2 (THEMIS)
HCG 92e	-	0.01±0.01	0.01±0.01	0.03±0.01	64.57	100
SQ-A	-	0.46±0.02	0.46±0.02	-	-	100
SQ-B	0.01±0.01	0.13±0.01	0.13±0.01	-	-	100

(1) Star-formation rate derived from UIR 6.2 μm band luminosity (Shipley et al. 2016).

(2)&(3) Star-formation rate calculated from 8–1000 μm luminosity (Shipley et al. 2016).

(4) Star-formation rate derived from MAGPHYS. The values are retrieved from Bitsakis et al. (2011). The error was not given by authors. Therefore, we adopted the maximum error of MAGPHYS refereed in da Cunha et al. (2008).

(5) Stellar mass derived from MAGPHYS. The values are retrieved from Bitsakis et al. (2011).

(6) Calculated by $L_{\text{SB}}/L_{\text{SB+AGN}}$. If the SED model does not take into account of the effect of AGN, the value becomes 100.

ACKNOWLEDGMENTS

This research is based on observations with AKARI, a JAXA project with the participation of ESA. This work is based in part on archival data obtained with the *Spitzer* Space Telescope, which is operated by the Jet Propulsion Laboratory, California Institute of Technology under a contract with NASA. Support for this work was provided by an award issued by JPL/Caltech. *Herschel* is an ESA space observatory with science instruments provided by European-led Principal Investigator consortia and with important participation from NASA. This work is supported by JSPS and CNRS under the Japan-France Research Cooperative Program and a grant for Scientific Research from the Japan Society for the Promotion of Science.

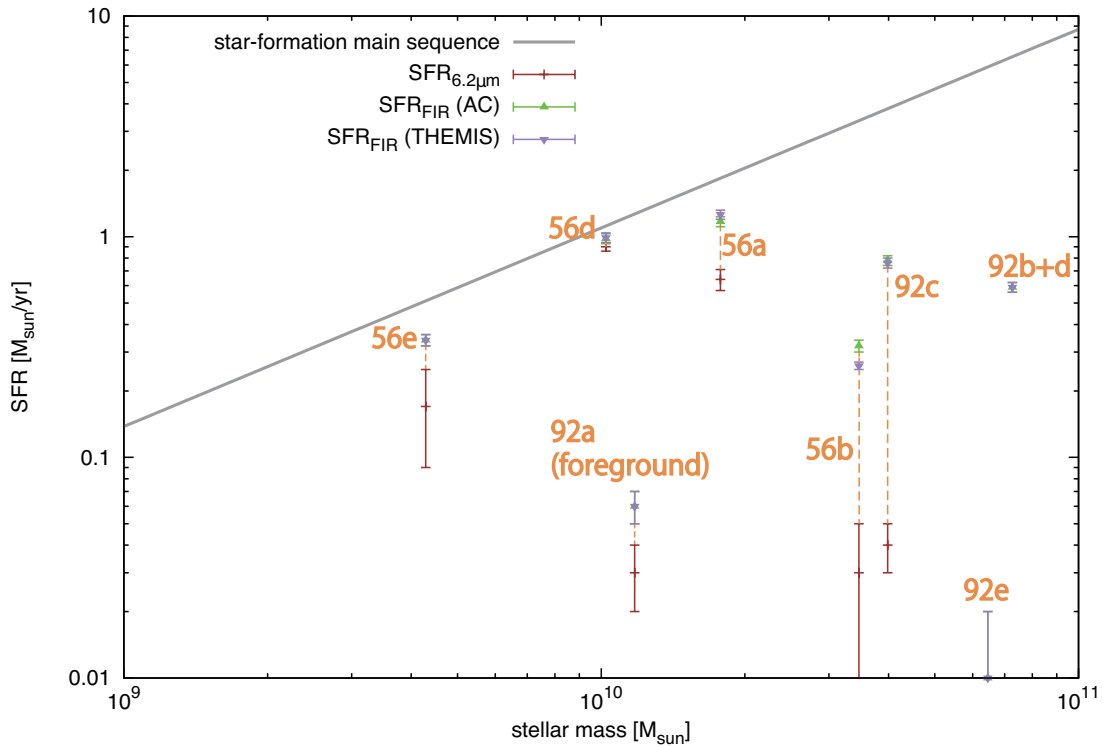


Figure 3. The SFR- M_{\star} relationship for star-forming SDSS galaxies ($z \sim 0.1$) of Brinchmann et al. (2004) (solid line) plotted with SFRs of our result and M_{\star} from the MAGPHYS fit (Bitsakis et al. 2011).

REFERENCES

- Bitsakis, T., Charmandaris, V., da Cunha, E., et al. 2011, *A&A*, 533, A142
 Brinchmann, J., Charlot, S., White, S. D. M., et al. 2004, *MNRAS*, 351, 1151
 da Cunha, E., Charlot, S., & Elbaz, D. 2008, *MNRAS*, 388, 1595
 Egusa, F., Usui, F., Murata, K., et al. 2016, *PASJ*, 68, 19
 Fazio, G. G., Hora, J. L., Allen, L. E., et al. 2004, *ApJS*, 154, 10
 Griffin, M. J., Abergel, A., Abreu, A., et al. 2010, *A&A*, 518, L3
 Galliano, F., Hony, S., Bernard, J.-P., et al. 2011, *A&A*, 536, A88
 Hickson, P. 1982, *ApJ*, 255, 382
 Jones, A. P., Fanciullo, L., Köhler, M., et al. 2013, *A&A*, 558, A62
 Kawada, M., Baba, H., Barthel, P. D., et al. 2007, *PASJ*, 59, S389
 Onaka, T., Matsuhara, H., Wada, T., et al. 2007, *PASJ*, 59, S401
 Poglitsch, A., Waelkens, C., Geis, N., et al. 2010, *A&A*, 518, L2
 Rieke, G. H., Young, E. T., Engelbracht, C. W., et al. 2004, *ApJS*, 154, 25
 Robitaille, T. P., & Whitney, B. A. 2010, *ApJL*, 710, L11
 Rubin, V. C., Hunter, D. A., & Ford, W. K., Jr. 1990, *ApJ*, 365, 86
 Shipley, H. V., Papovich, C., Rieke, G. H., Brown, M. J. I., & Moustakas, J. 2016, *ApJ*, 818, 60
 Siebenmorgen, R., Heymann, F., & Efstathiou, A. 2015, *A&A*, 583, A120
 Véron-Cetty, M.-P., & Véron, P. 2006, *A&A*, 455, 773